A Flowmeter for Measuring the Dispersed Phase Velocity in Multiphase Flow with Non-uniform Velocity Profiles

Sulaiyam Al-HINAI[1, 2] and Gary LUCAS[1]

[1] School of Department of School of Computing and Engineering Department, University of Huddersfield, Queensgate, Huddersfield HD1 3DH, UK

[2] Petroleum Development of Oman (PDO), Sultanate of Oman, P.O Box 81, Code 100, Sulaiyam Al-Hinai

Abstract

This study aims to introduce a new technique to measure the velocity distribution of the dispersed component of a vertical, upward, water continuous two-phase pipe flow. Here, it is proposed that measurements of the variation in the local conductance of the mixture can be cross correlated to determine the local velocity distribution of, for example, gas bubbles in water.

The measurements were conducted by using arrays of axially separated conductance sensors placed normal to the flow. Each array contained eight electrodes distributed over the internal circumference of the pipe carrying the flow. The arrays, were mounted at a known distance from each other along the pipe. Within each array, individual electrodes could be configured as either 'excitation', 'measurement' or 'earth'. By changing the electrode configuration of an array the electric field sensitivity distribution associated with the array could be altered, thus changing the region of the flow 'interrogated' by the system. By cross correlating the output signals from these arrays, in various combinations, the velocity of the dispersed phase can be obtained at different regions within the flow, thereby enabling the velocity profile of the dispersed phase to be measured.

The sensitivity distribution associated with given electrode configurations has been investigated in a bench test. First the flow meter was filled with water, and then non-conducting rods were inserted into the flow meter at various spatial locations parallel to the pipe, the resulting change in conductance was measured.. The sensitivity distribution has also been simulated using COMSOL software. Agreement between experiment and theory was close to 1 %.

Key words

Multiphase Flow, Conductance Sensors, Cross-correlation, Velocity Profile, COMSOL 2D and 3D Simulation

1. Introduction

Multiphase flows, where two or three fluids may flow simultaneously in a pipe are important in many applications within oil, mining, paper pulp, natural gas and other industries. It is vital for these industries to precisely monitor the flows properties, such as the mean volume fraction (α_i) and mean velocity (V_i) of each phase to quantify the flow rate, as:

$$Q_i = \alpha_i V_i A \qquad (1)$$

where: A is the cross-sectional area of the pipe.

Traditional commercial measuring techniques employ bulky, heavy and expensive separators to separate the mixture into its various components and meter them individually, which is time consuming and not suitable for continuous monitoring.

A major problem for the measurement of multiphase flow is that it can occur in a number of different, not necessarily clearly defined, regimes such as stratified or dispersed or annular or slug [1], which require different measurement techniques. For example for a homogeneous multiphase flow, a single phase flow measurement technique may sometimes be used; whilst in the slug regime, where the flow is transient and intermittent, single phase techniques cannot be applied. Furthermore, a complex two-way coupling between the two phase flow pattern and the geometry of the containing pipe, as well as the rates of change of that geometry, complicate the measurement. Pipe geometry variations due to bends, valves, and fittings, can disrupt the flow pattern over long distances (both upstream and downstream) before a stable pattern is once again established.

Today the measurement of volume fraction in multiphase flows has been largely resolved, but techniques for accurately measuring the mean velocity of each of the components are by no means so well developed. One of the most widely used techniques for velocity measurement in multiphase flow is spatial cross correlation (Figure 1).

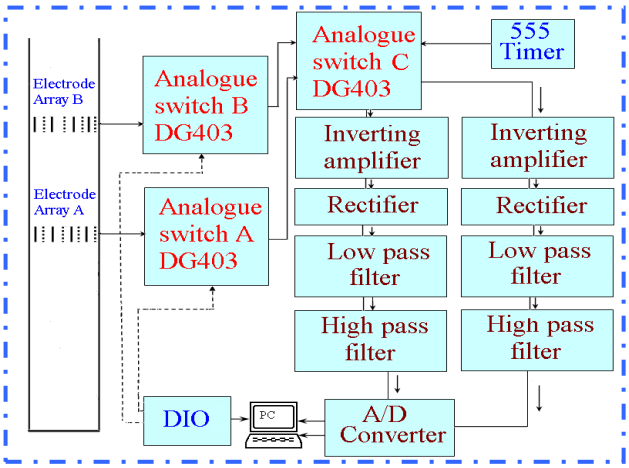

Fig 1: Schematic diagram of the data acquisition and control system.

This method remains under continuous development, see for example [1] and [2], but invariably they assume that some property of the flowing fluid, e.g. density, temperature, velocity, is changing in a random manner. This property is detected at two positions, A and B, on the

pipe and the corresponding detector output voltages are $x(t)$ and $y(t)$ .The cross-correlation function $R_{xy}(\tau)$ of the two random signals $x(t)$ and $y(t)$ is:

$$R_{xy}(\tau) = \lim_{T \longrightarrow \infty} \frac{1}{T} \int_0^T x(t-\tau) y(t) dt \qquad (2)$$

Where τ is a variable time delay and T is the time period over which the signals $x(t)$ and $y(t)$ are sampled. As the value of τ varies from 0 to T, the value of the cross correlation function $R_{xy}(\tau)$ will change, attaining a maximum value when τ is equal to τ_p the mean time for the perturbations in the relevant property of the flow to travel from A to B. Hence, τ_p can be found by determining the value of τ at which $R_{xy}(\tau)$ is a maximum. The average flow velocity $\bar{V}$ can be calculated, as:-

$$\tau_p = \frac{L}{\bar{V}} \qquad (3)$$

where: L is the distance between A and B (the electrode arrays). The aim of this investigation is to alter the electrode configurations at planes A and B to measure conductance variations in localized regions of the two planes. We can then cross-correlate the conductance variations in the two planes to estimate the mean local velocity of the dispersed phase in that region of the flow cross section. The overall mean flow velocity can then be calculated by appropriate combination of these local velocities.

2. Experimental Apparatus

The experimental apparatus used comprised an impedance cross-correlation (ICC) sensor system and a data acquisition system. The ICC sensor section was comprised of a non-conductive pipe section of 80mm internal diameter fitted with two arrays of electrodes at two planes, A and B separated by an axial distance of 50mm. At each plane eight electrodes were distributed over the internal circumference of the pipe (Fig 2). The electrode dimensions are 2.3mm long by 2mm high by 0.4mm deep. A control system consisting of a microcontroller and several analogue switches (Fig. 1) was used such that, for plane A, any of the eight electrodes could be configured as 'excitation electrodes' (V^+), 'virtual earth measurement electrodes' (ve) or 'earth electrodes' (E). The V^+ electrodes were connected to a sinusoidal excitation source with amplitude V_{in}. The ve electrodes were connected to the negative input of an inverting amplifier 'A' and the E electrodes were grounded (Fig 4). In this way, the fluid conductance $G_{f,a}$ between the V^+ and the ve electrodes could be measured since

$$V_{out,a} = -R_a G_{f,a} V_{in} \qquad (4)$$

where R_a is the feedback resistance of inverting amplifier 'A' (Fig. 4) and $V_{out,a}$ is the amplitude of the output voltage from amplifier 'A'.

A similar arrangement was used for plane B such that the fluid conductance $G_{f,b}$ between the V^+ and ve electrodes in plane B was obtained from the amplitude $V_{out,b}$ of the output voltage from inverting amplifier 'B' associated with plane B. Note that a switching mechanism involving the use of a 555 timer ensured that the V^+ electrodes in plane A and the V^+ electrodes in plane B were connected alternately to the excitation source. This meant that planes A and B were never active at the same time and so prevented 'cross talk' between the two planes. The switching frequency was 100kHz and the excitation signal applied to the V^+ electrodes was 10KHz and this resulted in the signals shown in Fig. 5 being applied to the V^+ electrodes in planes A and B. For any given test, at a particular angular electrode position (e.g. elec 1 in Fig 3) the electrodes in planes A and B were always of the same type (i.e V^+, ve or E). This meant that in any given test, the same region of the flow cross section was interrogated at planes A and B.

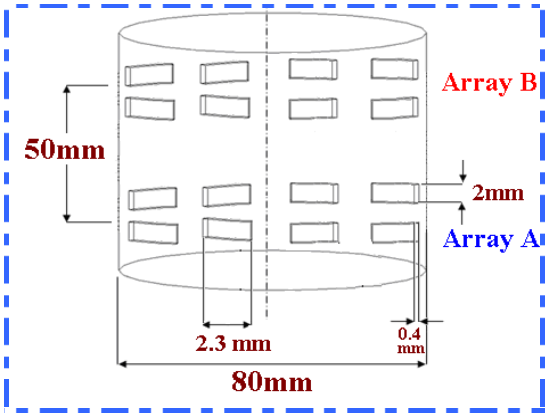

Fig 2: Arrangement of electrode array on the pipe

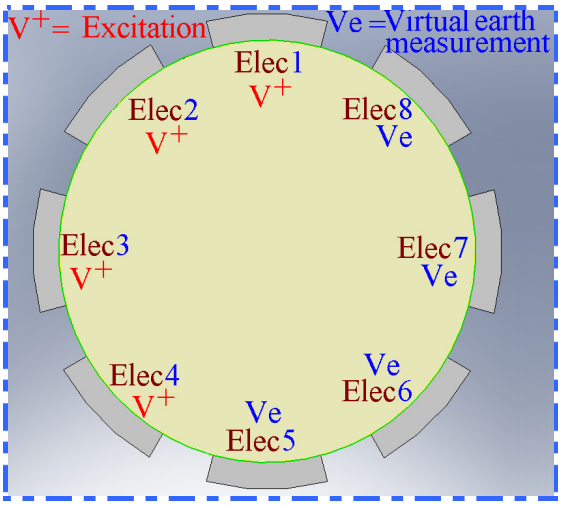

Fig 3: Array A electrode configuration

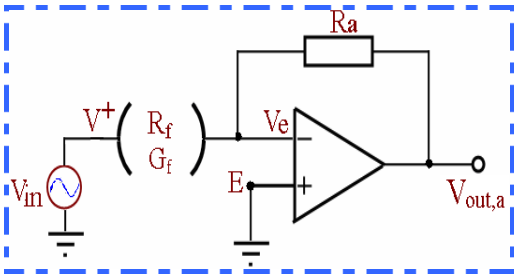

Fig 4: Fluid conductance circuit

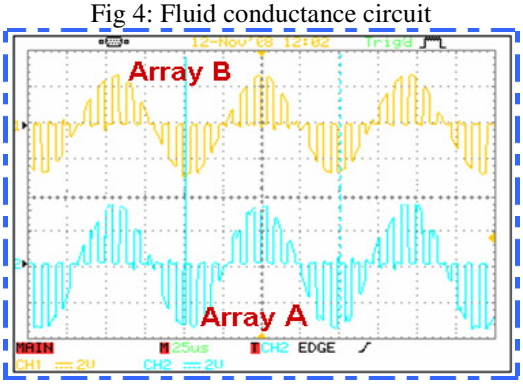

Fig 5: Excitation signals for excitation electrode in Array A & B

Signals $V_{out,a}$ and $V_{out,b}$ were each rectified and low pass filtered to produce d.c. output voltages V_a and V_b which could be subsequently cross correlated to provide information on the mean dispersed phase velocity (of a two phase flow) at the particular region of the flow cross section 'interrogated' by planes A and B. By changing which electrodes in planes A and B were V^+, ve or E electrodes, different parts of the flow cross section could be interrogated. A dedicated MATLAB 'm-file' module was used to perform cross correlation of the signals received from the two planes.

The data acquisition system shown in Fig. 1, is comprised of (i) DG403 analogue switches which enable computer control of the electrode configurations, (ii) an inverting amplifier, rectifier, low pass filter and high pass filter associated with each electrode plane; (iii) a USB based A/D converter for each plane and a USB based DIO unit for selecting the electrode configuration in each plane. In Fig. 1 analogue switch A is used to control the electrode configuration of the array A whilst analogue switch B is used to control the electrode configuration for array B. The purpose of using analogue switch array C is to ensure that the array A electrodes which are selected as V^+ excitation electrodes are not activated at the same time as the array B V^+ excitation electrodes, as described above. This is to prevent cross talk between the two electrode planes. Output signals V_a and V_b are sampled by the A/D converters which are connected to a PC for data recording and cross correlation.

3. Experimental Setup

By initializing the appropriate sampling and excitation frequencies, static bench tests were carried out to measure the sensitivity distribution inside the flow pipe. The purpose of these bench tests was to investigate spatial variations in the sensitivity of the electric 'sensing' field for a particular electrode configuration. It was intended that this investigation would provide insight into the best electrode configurations for measuring the 'local' dispersed phase velocity at particular regions within the flow cross section.

The circuit in the bench test setup was powered by ±15V, and the 10 KHz sine wave excitation signal of 1V peak to peak was provided by a laboratory signal generator. For each test, identical electrode configurations were selected for planes A and B. This electrode configuration was altered for each successive test. The circuit outputs V_a and V_b were fed into the A to D converter channels of a Labjack data acquisition device which was, in turn, connected to a PC. All the data analysis was done using MATLAB software.

Two plastic plates, each with 12 holes of equal diameter (15mm) were placed on the ends of the pipe forming the ICC flow meter. A long nylon rod, of 15 mm diameter, was inserted through one of the holes in the top plate. To ensure the rod was vertical and parallel to the walls of the pipe, its lower end sat in the second nylon plate at the bottom of the tube. These two plates were a distance of 470 mm apart. The holes in the plates were arranged as shown in figure 6. Since the geometry of the plates and their holes is known accurately, the position of the nylon rod in the flow cross section is also known. The position of each hole relative to electrodes '1' to '8' in each plane is shown in Fig. 6. The nylon rod was inserted into holes 1 to 12 in turn and the effect on the circuit output voltages V_a and V_b was investigated. It was found, as expected, that for a given electrode configuration, when the nylon rod was inserted into a given hole the changes in V_a and V_b were identical, consequently, in the next section, results associated with changes in V_a only are presented.

For a given electrode configuration, a sensitivity parameter $\delta V_{a,i}$ was defined such that $\delta V_{a,i} = V_{a,i} - V_{a,0}$ where $V_{a,i}$ is the value of the output voltage from the detection circuitry associated with plane A when the nylon rod is inserted into the i[th] hole and where $V_{a,0}$ is the value of this output voltage when the nylon rod was absent.

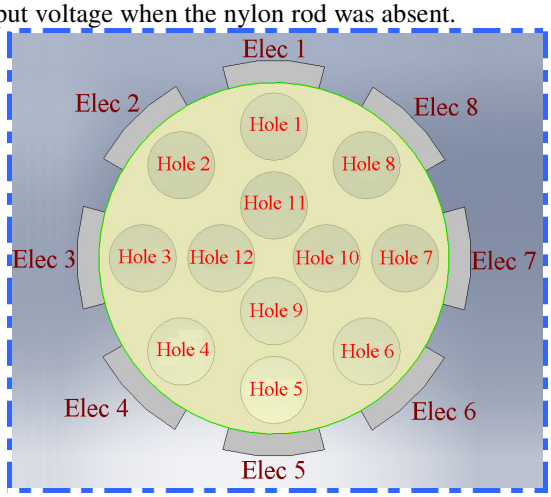

Fig 6: A 12 holes associated with different electrode

4. Experimental Results and Discussions:

4.1 Electrode Configurations 1 &2

The first and second test configurations are summarized in Table 1.

Table 1: Test Configurations 1& 2

Electrode configuration	Config-1	Config-2
	Electrode number	Electrode number
Excitation (V^+)	3,4,5,6	4,5,6
Virtual Earth (ve)	1,2,7,8	1,2,7,8
Earth (E)	none	3

The sensitivity distribution of configurations 1 and 2 is shown in figure 7 (a),(b). The vertical axis in figure7 (a),(b) represents the sensitivity parameter $\delta V_{a,i}$ (also represented by the colour scale to the right of the diagram).

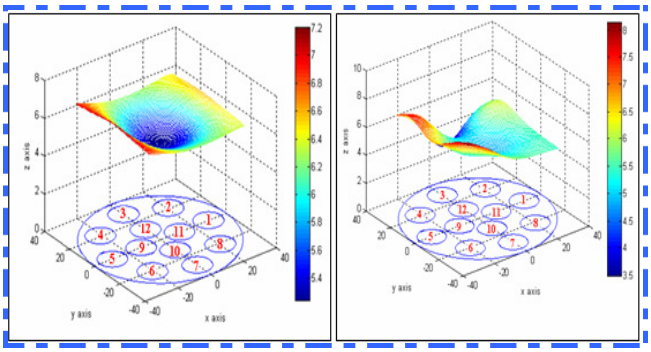

(a) Config-1 (b) Config-2

Fig 7: Sensitivity distributions

It is clear from Fig 7 (a) that for configuration 1 the system sensitivity in the vicinity of electrodes (3,4,5,6) is somewhat higher than the sensitivity in the vicinity of electrodes (1,2,7,8). The lowest sensitivity was at the middle of the pipe. Nevertheless, the sensitivity distribution for configuration 1 is relatively uniform in the flow cross section.

Fig 7 (b) shows the sensitivity distribution for configuration 2. In the vicinity of electrodes (4, 5, 6) the sensitivity is high compared with the sensitivity in the vicinity of electrodes (1,2,7,8). However, the sensitivity in the vicinity of electrode (3) was low. This is due to the fact that (3) is a grounded electrode.

4.2 Electrode Configurations 3 & 4

The summaries of the electrode configurations 3 and 4 are shown in Table 2.

Table 2: Test Configurations 3 &4

Electrode configuration	Config-3	Config-4
	Electrode number	Electrode number
Excitation (V^+)	1	5
Virtual Earth (ve)	2,8	1
Ground (E)	3,4,5,6,7	2,3,4,6,7,8

The system sensitivity for configurations 3 and 4 are shown in figure 8 (a),(b) . The vertical axis in figure 8 (a), (b) again represents the sensitivity parameter $\delta V_{a,i}$ (also represented by the colour scale to the right of the diagram).

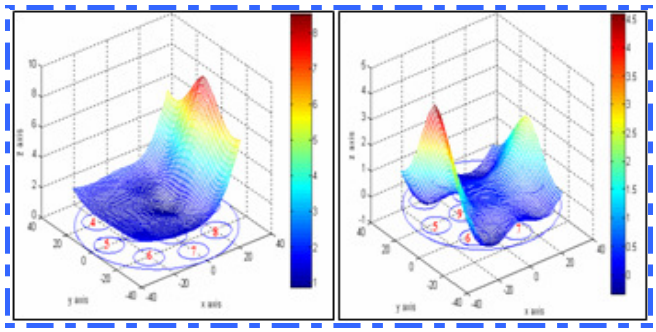

(a) Config-3 (b) Config-4

Fig 8: Sensitivity distributions

From Fig 8 (a), the lowest system sensitivity was in the vicinity of the ground electrodes (3,5,6,7,8). There is higher sensitivity in the vicinity of electrodes (1,2,8) but it can be seen that the system sensitivity is much higher in the vicinity of electrode (1) compared with electrodes (2,8) . Fig 8 (b) shows that the system sensitivity in the vicinity of the excitation electrode (no.5) is again higher than for the other electrodes while the sensitivity at grounded electrodes was very small.

4.3 Electrode Configurations 5 & 6

The summary of electrode configurations 5 and 6 is given in Table 3.

Table 3: Test Configurations 5&6

Electrode configuration	Config-5	Config-6
	Electrode number	Electrode number
Excitation (V^+)	1	6
Virtual Earth (ve)	8	5
Ground (E)	2,3,4,5,6,7	1,2,3,4,7,8

The system sensitivity of configuration 5 and 6 is shown in figure 9 (a), (b).

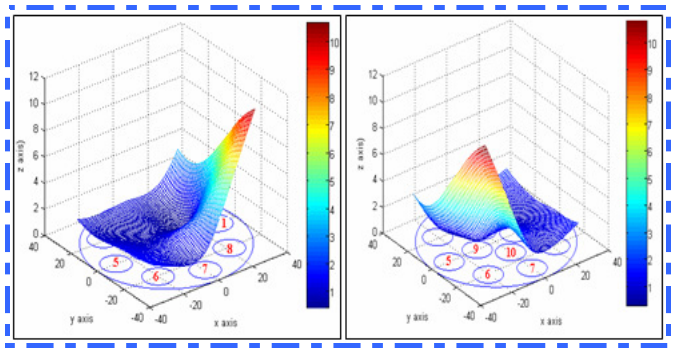

(a) Config-5 (b) Config-6

Fig 9: Sensitivity distributions

It is clear from Fig 9 (a) that the system sensitivity in the vicinity of electrode (1) is much higher than elsewhere in the flow cross section. The lowest sensitivity was in the vicinity of grounded electrodes (2,3,4,5,6,7). The sensitivity distribution associated with configuration 6 is

expected to be the same as that for configuration 5 except that it is rotated clockwise by 135 ^{o}. The experimental results shown in figure 9 (a),(b) confirm this expectation. Thus, from figure 9 (a), (b) it is apparent that if we set one electrode as V^+, an adjacent electrode as ve and all of the other electrodes as E, then we will interrogate the flow in a relatively 'local' region adjacent to the V^+ electrode.

5. Finite-element Models

A model of a 'single plane', 8-electrode sensor has been produced, using a two dimensional finite element model developed using COMSOL, and was used to calculate the sensitivity distribution for different electrode configurations.

The results from COMSOL were compared with experimental results obtained for Configuration-1 (see table-1 for electrode configuration). Fig 10 shows the results obtained from COMSOL for the same electrode configuration as the experimental results shown in figure 7 (a) (section 4.1).

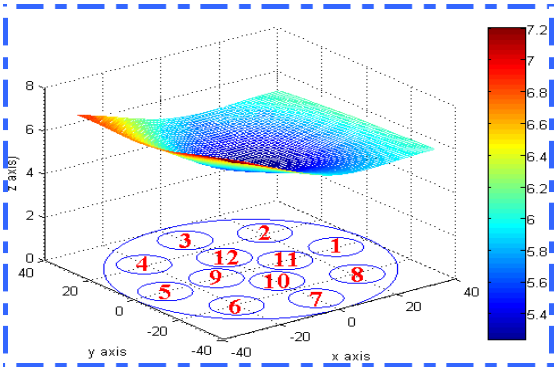

Fig 10: Result from COMSOL (same as the result from Configuration 1 section 4.1)

Comparing Fig 10 with Fig 7 (a), it can be concluded that the error between the theoretical and experimental results is very small. This error is shown in Fig 11. The vertical axis in Fig 10 represents the change in voltage when a nylon rod is inserted in the given hole whose number is indicated on the horizontal axis. The theoretical and experimental results are within about 1% of each other.

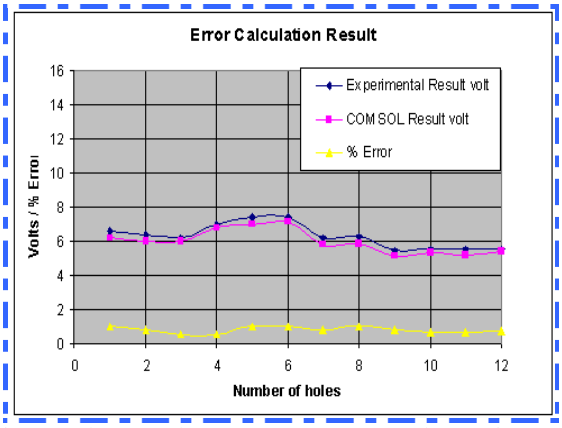

Fig 11: The error between COMSOL and experimental result

6. Dynamic Tests on ICC System

In this experiment two balls were used which have the same diameter of 29mm but different densities (1200kg/m^3, 1164.7 kg/m^3 for balls P and Q respectively) in order to examine the velocities of the two balls. Firstly, we set the electrode configuration for arrays A and B to Configuration 5 (Table 3). The balls were dropped at the same time but in different parts of the pipe; ball P was dropped between electrodes 1&8 and ball Q was dropped between electrodes 5 & 6 as shown in Fig 12. Then, the signals V_a (red) and V_b (blue) from the two arrays were measured and cross correlated as shown in figure 14.

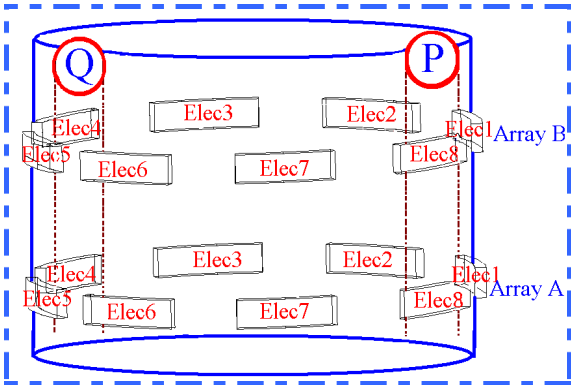

Fig 12: Arrangement of electrode array on the pipe

It is clear from Fig. 13 that the system was only sensing ball P, whereas ball Q produced no noticeable effect on the output voltages V_a and V_b. This is because (with reference to Fig. 9 (a)), for electrode configuration 5, the sensitivity of the electric 'sensing field' close to electrodes '1' and '8' (the location of ball P) is much higher than the sensitivity close to electrodes '5' and '6' (the location of ball Q). Thus, we see that for electrode configuration 5 the ICC system preferentially detects velocities in that part of the flow cross section close to electrodes '1' and '8'. Cross correlating V_a and V_b gives rise to the single peaked correlogram shown in figure 14 with the peak value at a time delay of 0.04 seconds. Given that the axial separation of the arrays is 0.05m, this corresponds to a measured velocity of 1.2ms^{-1}. Reference velocities for the balls were assumed to be their terminal velocities V_T given by the expression

$$V_T = \left[\frac{4}{3} d \left(\frac{\rho_B - \rho_w}{\rho_w} \right) \frac{g}{C_D} \right]^{0.5} \qquad (5)$$

where C_D is a drag coefficient for the ball, dependent upon its shape and surface roughness properties. In the current investigation a value of C_D equal to 0.059 was employed for both balls P&Q. Equation 5 is obtained by assuming that the gravitational force on the ball in the downwards direction is equal to the drag and buoyancy forces on the ball in the upwards direction when the ball is traveling at its terminal velocity V_T [7]. It can be seen

from equation (5) that V_T is dependent upon the ball diameter d. Also in equation (5) ρ_w is the density of the water ρ_B is the ball density and g is the acceleration of gravity. From equation (5) the reference velocity of ball P was 1.286ms^{-1}.

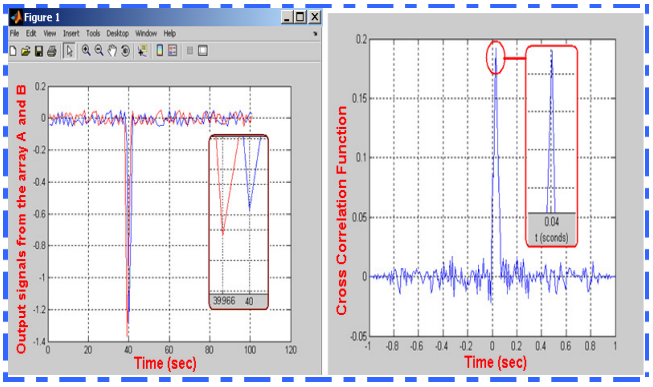

Fig 13: The output signals from array A & B

Fig 14: The cross-correlation from the two signals

Next the electrodes in arrays A and B were set to configuration 6 (see Fig 8 (b)). For this test the sensitivity of the electric field was much higher in the vicinity of ball Q than in the vicinity of ball P. The test was repeated as above and again a single peaked correlogram was produced with the peak value at a time delay of 0.0505 seconds. This corresponds to a measured velocity of 0.99ms^{-1}. From equation (5) the expected velocity of ball Q was 1.029ms^{-1}. This confirms, as expected, that for configuration 6, the ICC system only senses flow velocities in the vicinity of electrodes 5 and 6.

Finally, the electrode configuration for arrays A and B was set to configuration 1 (Table 1), which gives rise to a relatively uniform sensing field. Again, the balls were dropped at the same time, with ball P dropped between electrodes 1 & 8 and ball Q dropped between electrodes 5 & 6. Voltages V_a (red) and V_b (blue) were obtained from arrays A and B respectively as shown in Fig 15.

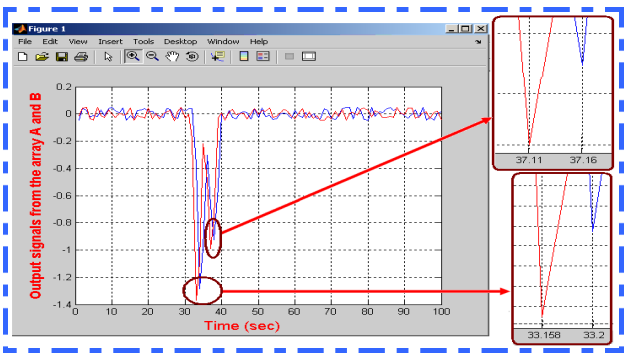

Fig 15: The output signals from array A&B

It can be seen from Fig 15 that two spikes occur in both V_a and V_b the first associated with ball P the second associated with ball Q. By zooming in Fig 15, the time taken by the two balls to pass the two electrode arrays (A, B) can be determined.

Table 4: Delay time obtained from cross-correlation function and the velocity for ball P&Q

	Time (s)	Velocity (m/s)
Ball P	0.042	1.19m/s
Ball Q	0.051	0.99m/s

The velocities in table 4 correspond closely to the measured velocities for P and Q when they were sensed individually (see above). It is therefore apparent that, for configuration 1, the electric field is sensitive to the presence of the balls in all parts of the flow cross section.

7. Conclusions

It can be seen from the results presented above that the area of the flow cross section 'interrogated' by the ICC device is highly dependent upon the electrode configuration and that it is possible to have some configurations which interrogate specific localized regions of the flow whilst other configurations interrogate the entire flow cross section.

Using the results of the research presented in this paper it is intended in the future to use the ICC to 'map' the local velocity distribution of the dispersed phase in water-continuous two phase flows with highly non-uniform velocity distributions. The spatial resolution of this velocity mapping will be of the same order of size as the region of 'maximum sensitivity' for a given electrode configuration e.g. as shown in Fig. 9(a).

8. References

[1] X Deng, F Dong, L J Xu, X p Liu and LA Xu: *The design of a dual-plane ERT system for cross correlation measurement of bubbly gas/liquid pipe flow* ***Meas. Sci. Technol.*****12** (2001) 1024-103.

[2] GP Lucas and N D Jin: *Measurement of the homogeneous velocity of inclined oil-in-water flows using a resistance cross correlation flow meter* ***Meas. Sci. Technol.*** **12** (2001) 1529-1537.

[3] Beck M S and Plaskowski A: *Cross Correlation Flowmeters. Their Design and Application.* Bristol: Hilger (1987).

[4] Lucas GP, Cory JC, Waterfall R C, Loh W and Dickin F J : *Measurement of the solids volume fraction and velocity distributions in solids-liquids flows using dual-plane electrical resistance tomography.* **J**. **F**low **M**eas. **I**nstrum. **10** (1999) 249-58.

[5] Greg A. Oldenborger, Parta S. Routh and Michael D.knoll: *Sensitivity of electrical resistivity tomography data to electrode position errors.* **G**eophys. **J**. **I**nt. **163** (2005), 1-9

[6] Cory J: *The measurement of the volume fraction and velocity profiles in vertical and inclined multiphase flows* , PhD Thesis University of Huddersfield (2000).

[7] Govier G and Aziz K: *The Flow of Complex Mixtures in pipes,* Van Nostrand Rheinhold (1972).